Scaling Laws of the Two-Electron Sum-Energy Spectrum in Strong-Field Double Ionization

Difa Ye,[1] Min Li,[2,3] Libin Fu,[1,4] Jie Liu,[1,4,5,*] Qihuang Gong,[2,3] Yunquan Liu,[2,3,†] and J. Ullrich[6,7]
[1]Institute of Applied Physics and Computational Mathematics, Beijing 100088, People's Republic of China
[2]Department of Physics and State Key Laboratory for Mesoscopic Physics, Peking University, Beijing 100871, People's Republic of China
[3]Collaborative Innovation Center of Quantum Matter, Beijing 100871, People's Republic of China
[4]CAPT, HEDPS, and IFSA Collaborative Innovation Center of MoE, Peking University, Beijing 100871, People's Republic of China
[5]Center for Fusion Energy Science and Technology, China Academy of Engineering Physics, Beijing 100088, People's Republic of China
[6]Max-Planck-Institut für Kernphysik, Saupfercheckweg 1, 69117 Heidelberg, Germany
[7]Physikalisch-Technische Bundesanstalt, Bundesallee 100, 38116 Braunschweig, Germany
(Received 15 January 2015; published 15 September 2015)

The sum-energy spectrum of two correlated electrons emitted in nonsequential strong-field double ionization (SFDI) of Ar was studied for intensities of 0.3 to 2×10^{14} W/cm^2. We find the mean sum energy, the maximum of the distributions as well as the high-energy tail of the scaled (to the ponderomotive energy) spectra increase with decreasing intensity below the recollision threshold (BRT). At higher intensities the spectra collapse into a single distribution. This behavior can be well explained within a semiclassical model providing clear evidence of the importance of multiple recollisions in the BRT regime. Here, ultrafast thermalization between both electrons is found occurring within three optical cycles only and leaving its clear footprint in the sum-energy spectra.

DOI: 10.1103/PhysRevLett.115.123001 PACS numbers: 32.80.Rm, 31.90.+s, 32.80.Fb, 32.80.Wr

The energy spectrum of photoelectrons has contributed much to our present knowledge about the basic dynamical mechanisms of strong-field ionization, and thus, has received constant attention during the past decades. These spectra are found to strongly depend on the laser parameters even when only one electron is removed from the atoms or molecules. In the low-intensity and short-wavelength region, the Keldysh parameter γ [1] ($\gamma = \sqrt{I_p/2U_p}$; I_p is the ionization potential; $U_p = \varepsilon_0^2/4\omega^2$ is the ponderomotive energy with ε_0 and ω denoting the laser field amplitude and angular frequency, respectively; atomic units are used throughout the paper unless otherwise specified) is much larger than 1. Here, above-threshold ionization is observed as one of the prominent phenomena where a photoelectron can absorb substantially more photons than the minimum number required for ionization, resulting in a typical energy spectrum consisting of several peaks that are separated by one photon energy $\hbar\omega$ [2]. Switching to the limit at high field and long wavelength (i.e.,$\gamma \ll 1$), the energy spectrum develops into another common pattern: a sharply decreasing slope from 0 to $2U_p$ is followed by a prominent plateau, and again a sharply decreasing slope cuts off the distribution at about $10U_p$ [3,4]. The classical model reveals that $2U_p$ is the maximum energy that can be obtained by a photoelectron which is directly accelerated away after tunneling by the electromagnetic field. If, however, the photoelectron is thrown back and gets backscattered upon its parent ion, its kinetic energy can be boosted up to $10U_p$ [5].

For SFDI, the issue becomes more complicated due to the correlated-electron dynamics involved [6]. Its general features have been most advantageously revealed in the past by inspecting the correlated electron momentum spectra. Here, the momentum components along the laser polarization direction of both electrons that are detected in coincidence are plotted in a two-dimensional representation. In general one observes emission into one hemisphere ("side-by-side") in the nonsequential region [7] and back-to-back emission (opposite hemispheres) below the recollision-threshold regime [8]. Moreover, in few electron-ion coincidence experiments, the photoelectron energy spectrum for SFDI has been inspected as well [9–12]. The sum energy of two electrons is a very global observable, which has the advantage that contains the whole information of the system including both the longitudinal (field-dominant) and the lateral (field-free) momenta of both electrons. This offers the unique possibility, in comparison with the popularly used correlation momentum plot between two electrons and the differential momentum plot of one individual electron, to study the system integratedly. The experiments indicate that photoelectrons for DI are more energetic (hotter) than for single ionization [12]. For multiphoton DI, the sum energy of two electrons is expected to reveal discrete peaks since the sum energy of two electrons is given by $E_1 + E_2 = n\hbar\omega - I_{p1} - I_{p2}$ (here, E_1 and E_2 are the continuum energies of the two electrons, and n is the number of absorbed photons. I_{p1} and I_{p2} are the Stark-shifted ionization potentials of the neutral

and the singly charged atom, respectively). Recently, it was indeed observed that the joint energy spectrum of two electrons emerging as a result of multiphoton DI of argon atoms at 400 nm reveals multiphoton ionization structure [13]. However, there are only very few studies published inspecting the sum energy of two electrons emerging from SFDI.

In this Letter, we experimentally and theoretically study the sum-energy spectra for SFDI of Ar at a wavelength of 800 nm. The calculations are performed for argon atoms and cover a wide range of laser intensities from 3×10^{13} to 2×10^{14} W/cm^2, crossing the recollision threshold and penetrating deeply into the BRT regime. Experimental distributions have been recorded at 4×10^{13}, 7×10^{13}, and 1.2×10^{14} W/cm^2. The most surprising finding is that the average sum energy as well as the high-energy tail of the distributions are *higher* in energy scaled to U_p for *lower* laser intensities and that the characteristics of the spectra change when crossing the BRT threshold. Above the threshold at 6×10^{13} W/cm^2, the normalized (plotting the sum energy in units of U_p) spectra almost collapse into a single curve. Below the threshold, however, the energy spectra significantly deviate from those in the above-recollision-threshold region, showing long tails up to $14U_p$. In both regimes, the profile of the spectra can be well fitted by a Γ-distribution function of the form $f(E) = cE^{\alpha}e^{-\beta E}$. The underlying physical mechanisms are discussed and revealed by means of both analytic deduction and inspection of the numerical statistics of the DI trajectories in Monte Carlo calculations.

Experimentally, we measured the sum energy of two electrons by an experimental setup including a high-power femtosecond laser oscillator operating with a repetition of 6 MHz [14] and a dedicated reaction microscope (REMI) [15]. In the REMI, the electrons and doubly charged ions generated from atoms of a supersonic jet in the tightly focused laser field were guided towards two position-sensitive delay-line equipped multichannel plate detectors by applying weak homogenous electric (2 V/cm) and magnetic (4.5 G) fields along the laser polarization direction. The laser polarization is oriented parallel to the time-of-flight direction of the spectrometer. Details of the setup, including information on the experimental resolution, have been published previously [14,15].

The measured sum-energy distributions of two electrons, normalized with respect to U_p, are shown in Fig. 1. One observes in Fig. 1(a) that the distribution at the lowest intensity (blue curve) of 4×10^{13} W/cm^2 exhibits a long tail extending to about $14U_p$ with a maximum of the distribution at around $5U_p$. Going to higher intensities the high-energy tail shrinks as well as the maxima of the distributions down to about $2U_p$ at 1.2×10^{14} W/cm^2. One can find that the line profile of the sum-energy distributions reveals the general feature of $f(E) = cE^{\alpha}e^{-\beta E}$. The fitted curves at 7×10^{13} and 4×10^{13} W/cm^2 are shown in Figs. 1(b) and 1(c),

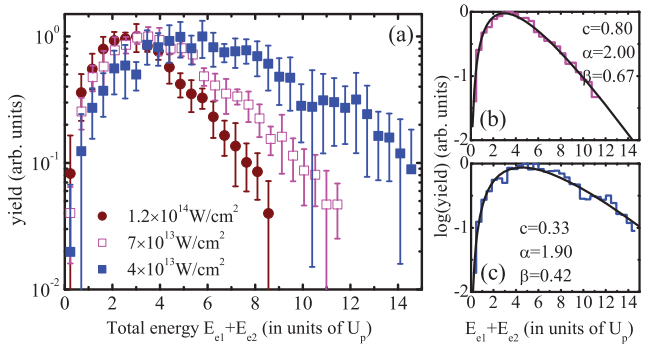

FIG. 1 (color). (a) The measured sum-energy distribution for SFDI at 800 nm and intensities of 4×10^{13}, 7×10^{13}, and 1.2×10^{14} W/cm^2. The sum energy is scaled with respect to U_p at each intensity and the maxima of the distributions are scaled to unity. In (b) and (c), the sum-energy spectra are fitted with the function of $f(E) = cE^{\alpha}e^{-\beta E}$ at 7×10^{13} and 4×10^{13} W/cm^2, respectively.

respectively. These findings are very different from the picture of multiphoton double ionization at 400 nm [13].

In order to extract the underlying dynamics generating these characteristics of the sum-energy distributions, we have performed calculations using a three-dimensional (3D) semiclassical two-electron atomic ensemble model including tunneling for both electrons [16,17]. Briefly, in the model, the tunneled electron is released at the outer edge of the field-suppressed Coulomb barrier through tunneling with a rate given by the ADK theory [18]. The bound electron is represented as a microcanonical distribution [19]. The subsequent evolution of the two electrons is governed by Newton's equations of motion: $d^2r_i/dt^2 = -\varepsilon(t) - \nabla_{r_i}(V^i_{ne} + V_{ee})$.Here, r is the spatial coordinate with the index i denoting the two electrons.$V^i_{ne} = -(2/|r_i|)$ and $V_{ee} = (1/|r_1 - r_2|)$ are the Coulomb interactions between the nucleus and both electrons and between two electrons, respectively. The laser field $\varepsilon(t)$ with a cosine waveform has constant amplitude for the first ten cycles and is turned off with a 3-cycle ramp. We consider the recollision induced excitation tunneling effect by allowing each electron to tunnel through the potential barrier whenever it reaches the outer turning point. When $p_{i,z} = 0$ and $z_i\varepsilon(t) < 0$, the tunneling probability P^{tul}_i is given by the Wentzel-Kramers-Brillouin (WKB) approximation $P^{\mathrm{tul}}_i = \exp[-2\sqrt{2}\int_{z^{\mathrm{in}}_i}^{z^{\mathrm{out}}_i} \sqrt{V(z_i) - V(z^{\mathrm{in}}_i)}dz_i]$ [17,20], where z^{in}_i and z^{out}_i are the two roots ($|z^{\mathrm{in}}_i| < |z^{\mathrm{out}}_i|$) of the equation for z_i, $V(z_i) = -2/r_i + z_i\varepsilon(t) = -2/r^{\mathrm{in}}_i + z^{\mathrm{in}}_i\varepsilon(t)$. In the calculation, the first and second ionization potentials are chosen as $I_{p1} = 0.58$ and $I_{p2} = 1.02$ a.u., respectively, to match the argon atoms. For more details of the theoretical methodology, please refer to Sec. IV D of Ref. [21] and references therein.

In Fig. 2, we show the calculated sum-energy distributions of argon atoms irradiated by an 800-nm laser

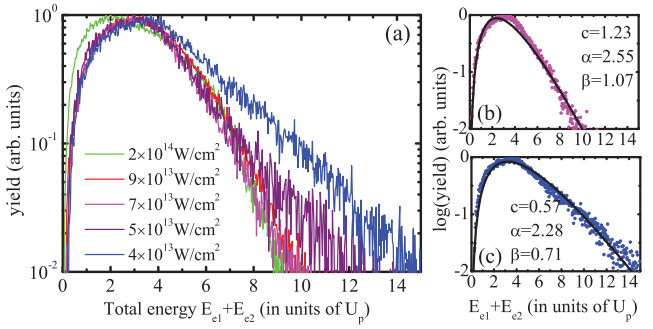

FIG. 2 (color). (a) The calculated sum-energy distribution for SFDI at 800 nm in the intensity region from 4×10^{13} to 2×10^{14} W/cm^2. In (b) and (c), the sum-energy spectra are fitted with the function $f(E) = cE^{\alpha}e^{-\beta E}$ at 7×10^{13} and 4×10^{13} W/cm^2, respectively.

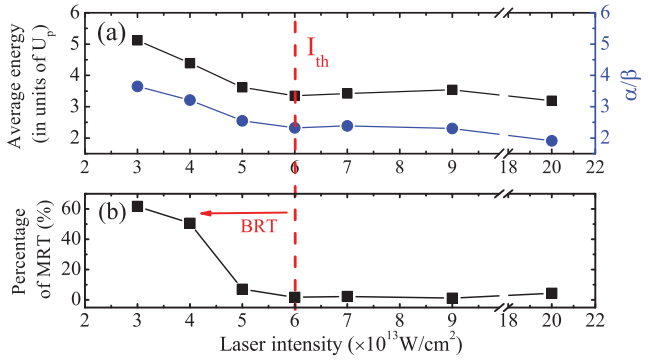

FIG. 3 (color). (a) Intensity dependence of the peak position of the theoretical sum-energy spectra (i.e., the parameter α/β, blue circles) and the arithmetic mean value of the sum energy (black squares). (b) The percentages of multiple-recollision trajectories (MRT). $I_{\mathrm{th}} = 6 \times 10^{13}$ W/cm^2 is the threshold intensity.

field with peak intensities varying from 3×10^{13} to 2×10^{14} W/cm^2. The calculated distributions reveal a similar line profile as observed in the experiment. Fitting the theoretical energy spectra in Fig. 2(a) with the Γ-distribution function $f(E) = cE^{\alpha}e^{-\beta E}$ [22], we obtain the parameters α and β for all intensities and the two spectra at 7×10^{13} and 4×10^{13} W/cm^2 corresponding to the experimental results [Figs. 1(b) and 1(c)] are presented in Figs. 2(b) and 2(c), respectively.

Then, we can obtain the maximum of the sum-energy distribution of the correlatively emitted electrons, using $df(E)/dE|_{E_{\mathrm{peak}}} = 0$, yielding to $E_{\mathrm{peak}} = \alpha/\beta$. The intensity dependence of this peak position is shown by the blue circles in Fig. 3(a). From these plots we see that the peak position is around $2U_p$ for laser intensities above 0.06 PW/cm^2 while, below 0.06 PW/cm^2, it rapidly increases with decreasing laser intensity. The intensity dependence of the average sum energy (i.e., the arithmetic mean) calculated directly from the spectra shown in Fig. 2(a) and illustrated as black squares in Fig. 3(a), display an analogous tendency indicating that the two fitting parameters α and β directly reflect the mean temperature of the system, which is controlled by the laser intensity.

The scaled sum-energy spectrum significantly broadens, extending well beyond $10U_p$ if one goes to lower intensities with the transition occurring at around the transition to the BRT regime. In comparison with sequential tunneling DI being the dominant DI mechanism in the above recollision threshold regime, field-assisted (multiple) electron recollisions of the first emitted electron are known to significantly enhance the ionization probability of the second electron. Here, during the recollision process, the returned electron changes phase and might then acquire even more energy from field, thus exhibiting higher final energy. As a consequence, the sum-energy spectra are expected to broaden due to the recollisions. The increasing broadening of the scaled energy spectra in the BRT regime might be expected to be a direct consequence of the increased number of multiple recollision trajectories.

This intuitive picture has been checked theoretically by inspecting the classical trajectories leading to DI. In our statistics for each trajectory, the number of recollision increases by 1 when two electrons become locally closest and fulfill two other conditions: (i) the two electrons approach each other to a relative distance of less than 3 a. u. with (ii) no other recollision occurring within a quarter of the laser cycle. In this way, we are able to identify those trajectories with no recollision, one recollision, or multiple recollisions. The result of this statistical analysis over the whole ensemble is plotted in Fig. 3(b). It exhibits a significant increase of the percentage of multiple recollision trajectories contributing to DI below about 6×10^{13} W/cm^2 up to about 60% at the lowest intensity investigated of 3×10^{13} W/cm^2, whereas such trajectories do not contribute at all above the threshold. Thus, on the basis of this analysis and observing a very similar tendency of the curves in Figs. 3(a) and 3(b), strong evidence is provided that multiple recollisions are responsible for the extension of the scaled sum-energy spectra to higher energies with decreasing intensity in the BRT regime.

To show how multiple recollisions facilitate the energy transfer from the tunneled electron to the bound one, we trace the evolution history of individual trajectories. Snap shots of this dynamics are presented in Fig. 4. Here we introduce the compensated energy $E_{ci} = -2/r_i + v_{ci}^2/2$ to filter out the temporal influence of laser field oscillation, where $v_{ci} = |\mathbf{r}_i - \int_t^{+\infty} \varepsilon(t')dt'|$ [19]. The snap shots show the evolution of the velocity distributions of both, the tunneled (black histogram) and the struck (red histogram) electrons, starting from $t = 0.75$ o.c. (optical cycle), i.e., the moment when the tunneled electrons are driven back to the parent ion. At this time, the tunneled electrons form a quasimonoenergetic bunch with energies as high as $3.17U_p$. In contrast, the struck electron has a much wider velocity distribution spanning over 3 a.u. [Fig. 4(a)]. The two electrons quickly exchange energy during recollision,

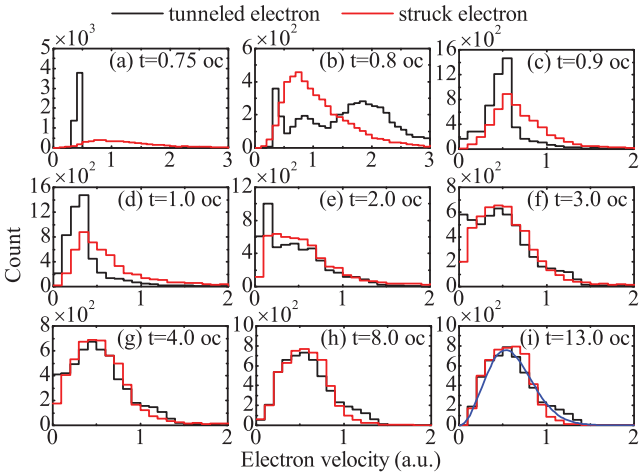

FIG. 4 (color). (a)–(j) Snapshots of the compensated-velocity distribution as time evolves from 0.75 o.c. to 13 o.c. For clear visualization, we only show those DI events triggered by tunneled electrons released at 17° of the cosine-shaped field. The laser intensity is 4×10^{13} W/cm^2. The blue curve in (i) is a Maxwell velocity distribution at the temperature of 4.5×10^4 K (3.9 eV), added by hand to guide the eye.

reaching a temporarily stable distribution within a short time scale of 0.15 o.c. (~400 as). After that, the evolution from $t = 0.9$ [Fig. 4(c)] to $t = 1.0$ o.c. [Fig. 4(d)] shows little adjustment in comparison with that from $t = 0.8$ [Fig. 4(b)] to $t = 0.9$ o.c. [Fig. 4(c)]. By this time, we have illustrated the effect of a single recollision. The effect of multiple recollision can be found by comparing the velocity distributions from cycle to cycle, as shown in Figs. 4(d)–4(i). As time evolves, multiple recollision facilitates the energy transfer between two electrons and gradually erases their difference in the velocity distribution. During the thermalization process the electrons are populated into doubly excited states and then ionized through over-the-barrier ionization or tunneling ionization sequentially with subsequent Coulomb scattering, which has already been discussed intensively in earlier papers [11,17].

What is even more interesting is the fact that the velocity distributions in the final stage are very close to Maxwellian distributions. This phenomenon is very similar to the thermalization of a many-particle closed system referring to the relaxation of an arbitrary initial energy (velocity) distribution towards a Maxwellian distribution via efficient energy exchange between particles. Here, in SFDI, this is facilitated by the repeated recollisions. Thermalization in nonsequential multiple ionization was discussed in Refs. [23,24] within an S-matrix-like model. Using this thermalization picture, the longitudinal momentum of doubly charged ions can be explained. However, it is only shown to work well at laser intensities above the recollision threshold. Our simulation with classical trajectories not only consolidates the thermalization picture but also reveals more details of the underlying mechanisms that are far beyond the capacity of the earlier papers. The plasma created in the focus volume of strong laser pulses that are long enough to enable multiple recollisions and weak enough to be in the BRT regime, can be treated as being in the thermodynamic equilibrium, which is reached within a very short time scale on the order of a few laser cycles only. All electrons in the volume are then at a universal temperature or exhibit the corresponding Maxwellian velocity distribution.

Now we provide some analytic arguments to explain the line shape of the energy spectrum and to reveal the physical meaning of α and β. An analytic expression for the sum-energy distribution in general is hard to be derived. As an enlightening example, we start from the deep BRT regime, and assume that the two electrons have reached the "thermal equilibrium" after the laser pulse is over. For relatively low intensities this is the case when the two electrons have undergone several soft recollisions and have had enough time to share their kinetic energy (as seen in Fig. 4). The energy distribution for each electron is assumed to follow the (3D) Boltzmann distribution, i.e.,$f(E_{1,2}) \sim \sqrt{E_{1,2}} e^{-\beta E_{1,2}}$. According to the general theory of statistics, the total energy distribution obeys $f(E = E_1 + E_2) = dF(E)/dE$, where $F(E) = \iint_{E_1+E_2<E} f(E_1) f(E_2) dE_1 dE_2$. After some simple deductions, we obtain that $f(E) \sim E^2 e^{-\beta E}$. Here, the analytically obtained parameter $\alpha = 2$ is found to be very close to the fitted ones as shown in Figs. 1(b), 1(c), and 2(b), and 2(c).

As to the fitting parameter β, let us elucidate the situation where sequential DI dominates, i.e., the high-intensity limit. In this case, the two electrons are deprived one by one from the ground state of Ar and Ar^+, respectively. Each ionization process is assumed to be in the tunneling regime and can be depicted well by the ADK theory (see, e.g., Ref. [25]). Thus, the probability for the ith electron entering the continuum at time t_i, with exponential accuracy, is $\varpi(t_i) \sim e^{-2\kappa_i^3/3\varepsilon_0|\cos(\omega t_i)|}$, where $\kappa_i = \sqrt{2I_{pi}}$. The tunneled electron is then accelerated by the laser field and finally acquires a drift energy $E_i = 2U_p \sin^2(\omega t_i)$. Combining the two processes, one obtains the energy distribution along the field direction $f(E_i) \sim e^{-2\kappa_i^3/3\varepsilon_0 \sqrt{1-E_i/2U_p}}$ [26]. The expression can be further simplified in the low-energy region $E_i \ll 2U_p$ as $f(E_i) \sim e^{-\beta_i E_i}$, with $\beta_i = 2\gamma_i^3/3\omega$ and γ_i is the Keldysh parameter for the ith electron. Following the same procedure presented in the above paragraph, we obtain the total energy distribution for sequential DI as $f(E) \sim (e^{-\beta_1 E} - e^{-\beta_2 E})/(\beta_2 - \beta_1)$. It reduces to $f(E) \sim E e^{-\beta E}$ when $\beta_1 = \beta_2 = \beta$ according to the l'Hôpital's rule. If the energy E is scaled with U_p, the parameter becomes $\beta_i' = \beta_i U_p = I_{pi}\gamma_i/3\omega = (I_{pi}/6\pi)\Delta t_{\mathrm{tul}}$, which is proportional to the tunneling time Δt_{tul} [1].

In conclusion, we have investigated the sum-energy spectra of two correlated electrons emitted in SFDI of argon atoms irradiated at 800 nm. We find that the scaled

sum energy of the two electrons reveal the general Γ-distribution. The macroscopic (statistical) and microscopic dynamics of electron thermalization occurring in SFDI was analyzed by a semiclasscial model. Specifically, we demonstrate that multiple recollisions strongly enhance the energy transfer between the tunneled electron and the bound one, thus facilitating the energy exchange between them, and leaving its footprint in the characteristics of the statistical distribution of the sum-energy spectrum.

We thank Dr. W. Becker for critical comments. Valuable discussions with Dr. A. B. Voitkiv and Dr. R. Moshammer are also acknowledged. This work is supported by the 973 programs (No. 2013CB922403 and No. 2013CB834100), the NSFC (No. 11434002, No. 11374040, No. 11304018, No. 11274051, No. 11134001, and No. 11125416), the Foundation of President of CAEP (No. 2014-1-029), and CAEP-FESTC (No. J2014-0401-03).

*liu_jie@iapcm.ac.cn
†yunquan.liu@pku.edu.cn

[1] L. V. Keldysh, Zh. Eksp. Teor. Fiz. **47**, 1945 (1964) [Sov. Phys. JETP **20**, 1307 (1965)].
[2] P. Agostini, F. Fabre, G. Mainfray, G. Petite, and N. K. Rahman, Phys. Rev. Lett. **42**, 1127 (1979).
[3] G. G. Paulus, W. Nicklich, H. Xu, P. Lambropoulos, and H. Walther, Phys. Rev. Lett. **72**, 2851 (1994).
[4] B. Walker, B. Sheehy, K. C. Kulander, and L. F. DiMauro, Phys. Rev. Lett. **77**, 5031 (1996).
[5] G. G. Paulus, W. Becker, W. Nicklich, and H. Walther, J. Phys. B **27**, L703 (1994); D. B. Milosevic and W. Becker, Phys. Rev. A **68**, 065401 (2003).
[6] B. Walker, B. Sheehy, L. F. DiMauro, P. Agostini, K. J. Schafer, and K. C. Kulander, Phys. Rev. Lett. **73**, 1227 (1994).
[7] Th. Weber, H. Giessen, M. Weckenbrock, G. Urbasch, A. Staudte, L. Spielberger, O. Jagutzki, V. Mergel, M. Vollmer, and R. Dörner, Nature (London) **405**, 658 (2000).
[8] Y. Liu, S. Tschuch, A. Rudenko, M. Dürr, M. Siegel, U. Morgner, R. Moshammer, and J. Ullrich, Phys. Rev. Lett. **101**, 053001 (2008).
[9] R. Lafon, J. L. Chaloupka, B. Sheehy, P. M. Paul, P. Agostini, K. C. Kulander, and L. F. DiMauro, Phys. Rev. Lett. **86**, 2762 (2001).
[10] J. L. Chaloupka, J. Rudati, R. Lafon, P. Agostini, K. Kulander, and L. F. DiMauro, Phys. Rev. Lett. **90**, 033002 (2003).
[11] X. Sun *et al.*, Phys. Rev. Lett. **113**, 103001 (2014).
[12] J. S. Parker, B. J. S. Doherty, K. T. Taylor, K. D. Schultz, C. I. Blaga, and L. F. DiMauro, Phys. Rev. Lett. **96**, 133001 (2006).
[13] K. Henrichs, M. Waitz, F. Trinter *et al.*, Phys. Rev. Lett. **111**, 113003 (2013).
[14] Y. Liu, S. Tschuch, M. Dürr, A. Rudenko, R. Moshammer, J. Ullrich, M. Siegel, and U. Morgner, Opt. Express **15**, 18103 (2007).
[15] J. Ullrich, R. Moshammer, A. Dorn, R. Dörner, L. Ph. H. Schmidt, and H. Schmidt-Böcking, Rep. Prog. Phys. **66**, 1463 (2003).
[16] B. Hu, J. Liu, and S.-g. Chen, Phys. Lett. A **236**, 533 (1997); L.-B. Fu, J. Liu, J. Chen, and S.-G. Chen, Phys. Rev. A **63**, 043416 (2001); D. F. Ye, X. Liu, and J. Liu, Phys. Rev. Lett. **101**, 233003 (2008).
[17] D. F. Ye and J. Liu, Phys. Rev. A **81**, 043402 (2010); Y. Liu, D. Ye, J. Liu *et al.*, Phys. Rev. Lett. **104**, 173002 (2010).
[18] M. V. Ammosov, N. B. Delone, and V. P. Krainov, Zh. Eksp. Teor. Fiz. **91**, 2008 (1986) [Sov. Phys. JETP **64**, 1191 (1986)].
[19] R. Abrines and I. C. Percival, Proc. Phys. Soc. London **88**, 861 (1966); J. G. Leopold and I. C. Percival, J. Phys. B **12**, 709 (1979).
[20] James S. Cohen, Phys. Rev. A **64**, 043412 (2001); K. I. Dimitriou, D. G. Arbó, S. Yoshida, E. Persson, and J. Burgdörfer, Phys. Rev. A **70**, 061401 (2004).
[21] W. Becker, X. Liu, P. J. Ho, and J. H. Eberly, Rev. Mod. Phys. **84**, 1011 (2012).
[22] The fitting is carried out with the least-squares method, i.e., minimizing the sum squared residuals $\sum |\log_{10}\sigma_E - \log_{10} f(E)|^2$. Here, σ_E is the energy spectra obtained with numerical simulation, and $f(E) = cE^{\alpha}e^{-\beta E}$ is the Γ-distribution function, in which α and β are two important structure factors, and c is a trivial normalization constant.
[23] X. Liu, C. Figueira de Morisson Faria, W. Becker, and P. B. Corkum, J. Phys. B **39**, L305 (2006).
[24] X. Liu, C. Figueira de Morisson Faria, and W. Becker, New J. Phys. **10**, 025010 (2008).
[25] S. Augst, A. Talebpour, S. L. Chin, Y. Beaudoin, and M. Chaker, Phys. Rev. A **52**, R917 (1995).
[26] V. P. Krainov, J. Phys. B **36**, L169 (2003).